NJC

Dynamic Article Links

Cite this: *New J. Chem.*, 2012, **36**, 781–788

www.rsc.org/njc

PAPER

Acid catalyzed coupling of aromatic aldehydes and methyldiazoacetate—a theoretical mechanistic study†

Georg Dazinger and Karl A. Kirchner*

Received (in Montpellier, France) 23rd September 2011, Accepted 21st December 2011
DOI: 10.1039/c2nj20824e

The proton catalyzed reaction of methyldiazoacetate and benzaldehyde resulting in the formation of β-ketoesters and 3-hydroxyacrylates has been investigated by means of DFT/B3LYP calculations. Experimentally this reaction is performed using $HBF_4{\cdot}Et_2O$ as the catalyst and CH_2Cl_2 as the solvent. Several mechanistic pathways involving 1,2-migration of phenyl-, H-, and OH-substituents have been considered. In agreement with the experiment, phenyl migration is slightly favored over H- and OH-migrations and thus the formation of 3-hydroxyacrylates over β-ketoesters takes place. Epoxide formation is not feasible in the presence of acid with non-nucleophilic counterions. Moreover, a counterion-assisted pathway has been also taken into account. The overall reaction is similar and competitive to the "BF_4^--free" pathway.

Introduction

Aromatic aldehydes are known to react with ethyldiazoacetate (EDA) in the presence of Lewis acids such as BF_3, $ZnCl_2$, $AlCl_3$, $GeCl_2$, and $SnCl_4$ to give mainly 3-oxo-3-arylpropanoic acid ethyl esters (β-ketoesters) (**I**) in high yields (Scheme 1).[1–3] 3-Hydroxy-2-arylacrylic acid ethyl esters (3-hydroxyacrylates) (**II**) were formed only as side products. It has to be mentioned that in none of these cases the formation of epoxides (**III**) was detected. The yield of **II** was improved significantly by utilizing $ZnCl_2$ in the presence of chlorotrimethylsilane as catalyst.[4] Hossain and co-workers have found that the cyclopentadienyl dicarbonyl Lewis acid $[FeCp(CO)_2(THF)]BF_4$[5] is an active catalyst for the coupling of aromatic aldehydes with EDA to afford **II** as the major product. Likewise, we have shown[6,7] that iron(II) PNP pincer complexes of the types $[Fe(PNP)(CO)(CH_3CN)_2](BF_4)_2$ and $[Fe(PNP)(CO)_2(Cl)]BF_4$ (PNP = *N*,*N*′-bis(diisopropylphosphino)-2,6-diaminopyridine) are efficient catalysts for this reaction affording almost exclusively **II**. Surprisingly, it was observed recently by Hossein *et al.* that even protons, in the form of Brønsted acids such as $HBF_4{\cdot}Et_2O$, catalyze the reaction between aromatic aldehydes and EDA to provide **I** and **II** in very good yields[8] with **II** being typically favored over **I**. It turned out, however, that Brønsted acids with poorly nucleophilic counterions such as BF_4^- were most efficient.[9] In fact, when the reaction was carried out with the acids HCl, H_2SO_4, $HClO_4$, HNO_3, and CH_3COOH instead of HBF_4, the yield was either poor or no reaction took place at all.

In the present paper we attempt to elucidate a reasonable mechanism for the HBF_4-catalyzed coupling process of aromatic aldehydes and EDA with benzaldehyde and methyldiazoacetate (MDA) as model compounds by means of DFT/B3LYP calculations. Issues to be addressed are the origin of the selectivity of the reaction, *i.e.*, β-ketoesters (**I**) *vs.* 3-hydroxyacrylates (**II**), the fact that epoxide formation (**III**) was not observed experimentally and the role, if any, of the counterion BF_4^-.

Computational details

All calculations were performed using the Gaussian09 software package on the Phoenix Linux Cluster of the Vienna University of Technology.[10] The geometry and energy of the model compounds and the transition states were optimized at the B3LYP level[11] with the 6-31G** basis set employed for all atoms.[12] All geometries were optimized without symmetry constraints. Frequency calculations were performed to confirm the nature of the stationary points, yielding one imaginary frequency for the transition states and none for the minima. Each transition state was further confirmed by following its vibrational mode downhill on both sides and obtaining the minima presented on the energy profiles. All energies reported are Gibbs free energies and thus contain zero-point, thermal, and entropy effects at 298 K and 1 atm pressure. The solvation energies were calculated on the geometries from B3LYP gas phase optimizations *via* the polarizable continuum model (PCM)[13] with the radii and nonelectrostatic terms based on Truhlar and co-workers' solute electron density (SMD) solvation model[14] with solvation parameters corresponding to CH_2Cl_2.

Institute of Applied Synthetic Chemistry, Vienna University of Technology, Getreidemarkt 9, A-1060 Vienna, Austria. E-mail: kkirch@mail.tuwien.ac.at; Fax: +43-1-58801-16399

† Electronic supplementary information (ESI) available: Cartesian coordinates and electronic energies, enthalpies, and free energies for all calculated compounds and transition states at the B3LYP/6-31G** level. See DOI: 10.1039/c2nj20824e

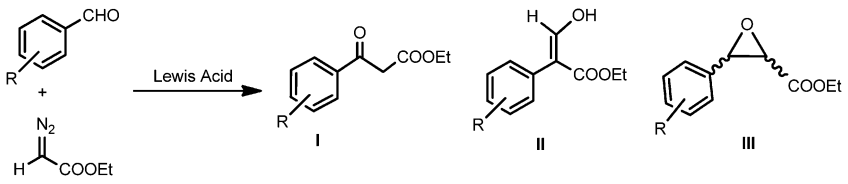

Scheme 1

NMR chemical shift calculations were obtained with the GIAO method at the B3LYP/6-311G** level. $SiMe_4$, calculated at the same level of theory, was used as reference to scale the absolute shielding values.

Results and discussion

Upon addition of $HBF_4{\cdot}Et_2O$ (10 mol% experimentally) to a solution of benzaldehyde in the aprotic solvent, CH_2Cl_2, the aldehyde oxygen atom is partially protonated affording both *Z* and *E* isomers ($\mathbf{A}^{Z}$, $\mathbf{A}^{E}$) as shown in Scheme 2. In agreement with experimental findings the *Z* isomer is slightly favored by 2.2 kcal mol^{-1}.[8,15,16] The barrier for an intramolecular *E*/*Z* isomerization is calculated to be 14.5 kcal mol^{-1} and is thus facile at room temperature. Double protonation at the oxygen

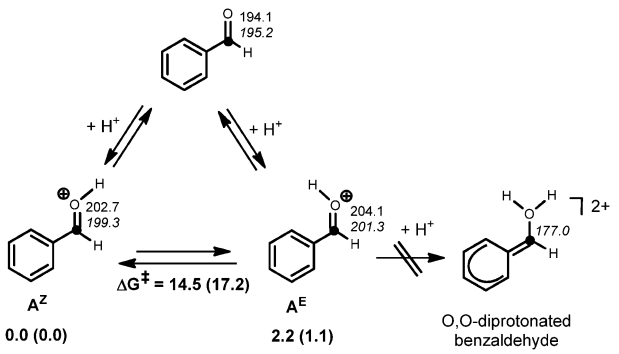

Scheme 2 Equilibria between free benzaldehyde, O-protonated benzaldehyde isomers, and O,O-diprotonated benzaldehyde (free energies in kcal mol^{-1}, experimental and calculated (*italic*) ^{13}C NMR chemical shifts δ in ppm relative to TMS, numbers in parentheses refer to solvent-corrected free energies, solvent = CH_2Cl_2).

to give an O,O-diprotonated benzaldehyde ion, as recently proposed in the literature,[8] is unlikely to occur. In fact, in the presence of super acids such as FSO_3H–SbF_6 it has been demonstrated that protonation of the arene ring rather than double O-protonation takes place. GIAO calculations based on the optimum DFT models of $\mathbf{A}^{Z}$, $\mathbf{A}^{E}$ and the O,O-diprotonated benzaldehyde have been performed revealing that ^{13}C NMR chemical shifts of the carbonyl carbon atoms were downfield shifted at 199.3 and 201.3 ppm, respectively. The values for the O-protonated benzaldehyde isomers are in good agreement with the experimental values (202.7 and 204.1 ppm, respectively).[8,16] There are no experimental data available for the ^{13}C resonances of an O,O-diprotonated benzaldehyde ion, which is considerably up-field shifted to 177.0 ppm as compared to benzaldehyde and the O-protonated benzaldehyde isomers.

Upon addition of MDA to a CH_2Cl_2 solution containing O-protonated benzaldehyde isomers, it is reasonable to assume that, at least to some extent, associated species such as $\mathbf{A_1}$, $\mathbf{A_2}$, and $\mathbf{A_3}$ are formed. In these species MDA is connected to O-protonated benzaldehyde isomers *via* hydrogen bonds as shown in Scheme 3. In fact, CH_2Cl_2 is a low-dielectric solvent with an ε of 8.9 and thus strongly promotes and facilitates electrostatic interactions. The formation of associates, particularly the formation of $\mathbf{A_3}^{Z}$ ($\mathbf{A_3}^{E}$), is thermodynamically very favorable and thus may play a role in the catalytic coupling reaction of aromatic aldehydes and MDA (*vide infra*).

Free energy profiles for the coupling of weakly associated O-protonated benzaldehyde $\mathbf{A_1}^{E}$ (the *Z*-isomer $\mathbf{A_1}^{Z}$ is slightly less reactive) and MDA *via si*- and *re* face attack are given in Schemes 4 and 5. Optimized structures of intermediates and transition states are depicted in Fig. 1. Calculated relative gas-phase enthalpies, free energies, and solvent-corrected free energies as well as activation enthalpies and free energies of activation for

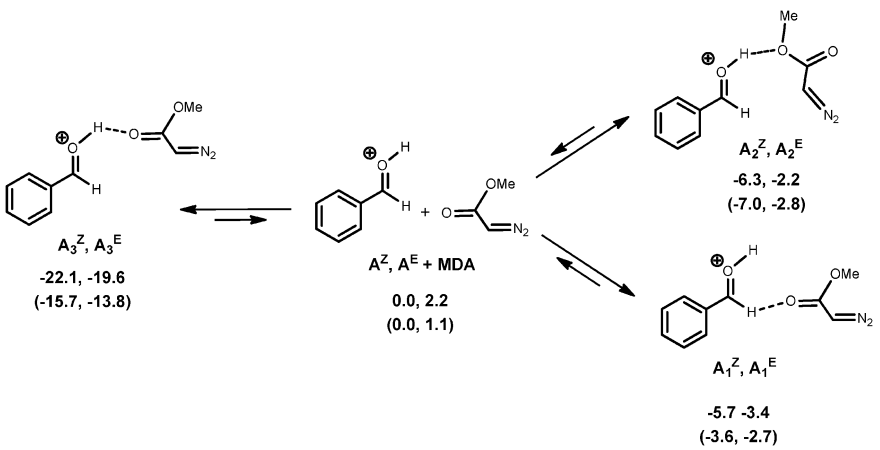

Scheme 3 Hydrogen bonding between O-protonated benzaldehyde *Z*/*E* isomers $\mathbf{A}^{Z}$, $\mathbf{A}^{E}$, and MDA forming associated species $\mathbf{A_1}$, $\mathbf{A_2}$, and $\mathbf{A_3}$, respectively (free energies in kcal mol^{-1}, numbers in parentheses refer to solvent-corrected free energies, solvent = CH_2Cl_2).

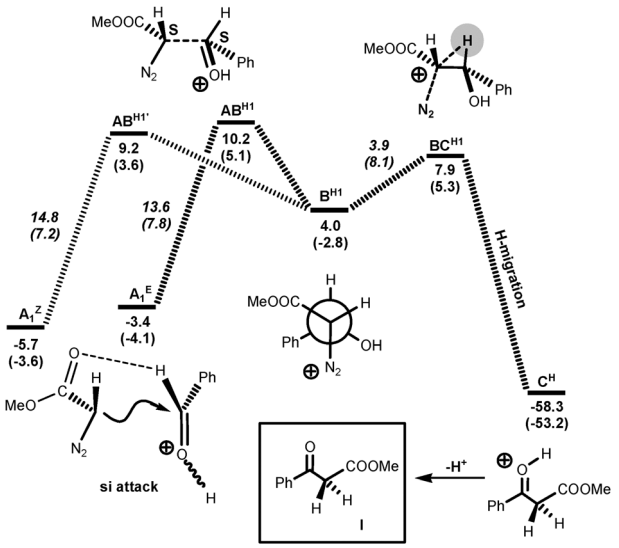

Scheme 4 Proton catalyzed coupling of O-protonated benzaldehyde and MDA *via si* face attack followed by H-migration to give β-ketoester **I**. The free energy values (kcal mol^{-1}) are referred to $\mathbf{A^Z}$ + **MDA** (separated O-protonated benzaldehyde and MDA), numbers in parentheses refer to solvent-corrected free energies, solvent = CH_2Cl_2.

all reaction steps are provided in Table 1. In the following paragraphs the gas phase energies are discussed. It has to be noted however that in all calculations solvent effects have been considered which typically lower the relative energies and energy barriers by 5–6 kcal mol^{-1} but do not change the overall mechanistic picture.

O-Protonation of benzaldehyde (or binding to strong Lewis acids, *e.g.* $[FeCp(CO)_2]^+$) increases the electrophilicity of the carbonyl carbon atom and facilitates nucleophilic additions of even rather weak nucleophiles such as MDA. Accordingly, nucleophilic attack of MDA at the *si*-face of the protonated aldehyde yields, *via* transition state $\mathbf{AB^{H1}}$, the diastereomeric intermediate $\mathbf{B^{H1}}$ adopting a 1*S*,2*S*-configuration (or the other enantiomer, *i.e.*, 1*R*,2*R*). In this compound the H and N_2 substituents are in an antiperiplanar position, a prerequisite for subsequent H-migration. This step is endergonic requiring 7.4 kcal mol^{-1}. The Gibbs free energy of activation is 13.5 kcal mol^{-1}. Once $\mathbf{AB^{H1}}$ is reached the changes associated with this step are already visible. The new C–C bond being formed is long (2.17 Å) indicating that the transition state structure occurs quite early along the reaction coordinate, while at the same time the C–N bond is elongated from the original MDA molecule (1.31 Å) with a C–N separation of 1.35 Å. The N_2-moiety is moving away from the original MDA molecule with a C–N bond distance of 1.77 Å. In $\mathbf{B^{H1}}$ the new C–C bond formed is 1.58 Å and the C–N bond is 1.45 Å.

Hydride migration (free energy of activation is 3.9 kcal mol^{-1}) leads to the O-protonated β-ketoester $\mathbf{C^H}$, passing through $\mathbf{BC^{H1}}$, and eventually upon proton loss to the β-ketoester **I**. In transition state $\mathbf{BC^{H1}}$ the C–C bond is slightly shortened (1.49 Å), while loss of N_2 is underway (d_{C-N} = 2.04 Å). At the same time, the shifting H-atom starts to move from the carbonyl C-atom (d_{C-H} = 1.12 Å) towards the adjacent carbon atom (d_{C-H} = 1.96 Å). The formation of $\mathbf{C^H}$ is strongly exergonic releasing 55.0 kcal mol^{-1}.

On the other hand, nucleophilic attack of MDA at the other enantioface (*re*-face) of the protonated aldehyde affords rotamer $\mathbf{B^{Ph2}}$ having an 1*S*,2*R*-configuration (or the other enantiomer) with the Ph substituent in an antiperiplanar orientation to the N_2 leaving group. This reaction, proceeding through transition state $\mathbf{AB^{Ph2}}$, is also endergonic (7.5 kcal mol^{-1}) with a free energy of activation of 14.4 kcal mol^{-1}. In $\mathbf{AB^{Ph2}}$, similar to

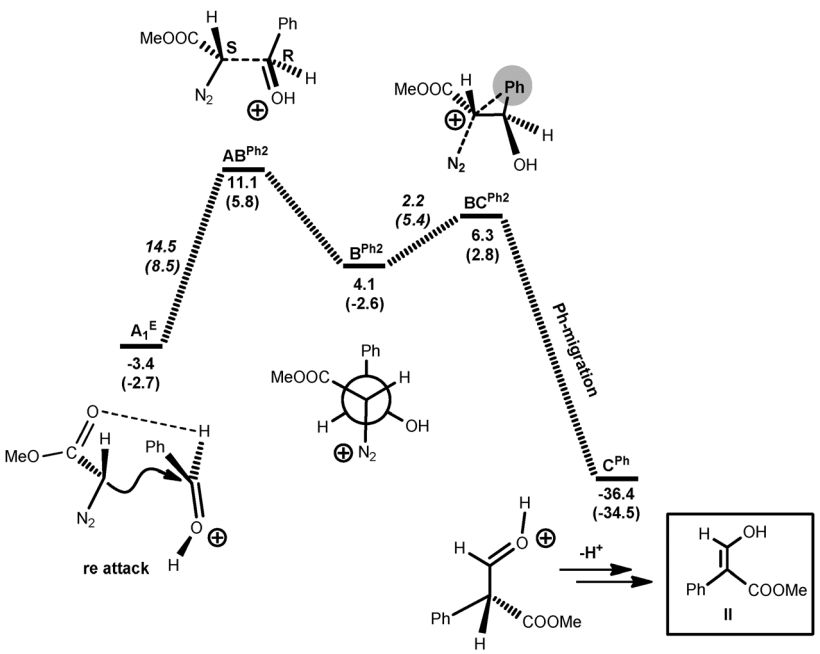

Scheme 5 Proton catalyzed coupling of O-protonated benzaldehyde and MDA *via re* face attack followed by Ph-migration to give hydroxyacrylate **II**. The free energy values (kcal mol^{-1}) are referred to $\mathbf{A^Z}$ + **MDA**, numbers in parentheses refer to solvent-corrected free energies, solvent = CH_2Cl_2.

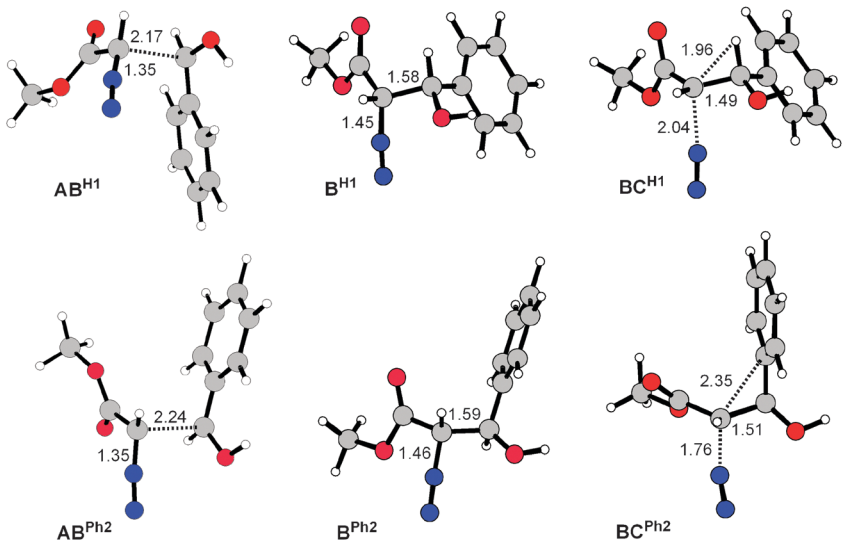

Fig. 1 Optimized B3LYP geometries of the equilibrium structures and transition states (distances in Å).

Table 1 Calculated relative gas-phase enthalpies, free energies, and solvent-corrected free energies, activation enthalpies and free energies of activation for the C–C bond forming, H-, Ph-, and OH-migration steps, respectively (kcal mol^{-1})[a]

Structure/reaction	ΔH	$\Delta H^{\ddagger}$	$\Delta\Delta H^{\ddagger}$	ΔG	$\Delta G^{\ddagger}$	$\Delta\Delta G^{\ddagger}$	ΔG_{sol}	$\Delta G^{\ddagger}_{sol}$	$\Delta\Delta G^{\ddagger}_{sol}$
A^{Z} + MDA	0.0			0.0			0.0		
A^{E} + MDA	2.3			2.2			1.1		
$A_1{}^{Z}$	11.2			−5.7			−3.6		
$A_1{}^{E}$	13.4			−3.4			−2.7		
$A_2{}^{Z}$	9.8			−6.3			−7.0		
$A_3{}^{Z}$	−6.6			−22.1			−15.7		
$A_1{}^{Z} \rightarrow AB^{H1\prime}$	22.3	8.9	4.0	9.2	14.8	3.1	3.6	7.2	3.0
$A_1{}^{E} \rightarrow AB^{H1}$	23.6	10.2	5.3	10.2	13.6	4.1	5.1	7.8	5.0
$A_3{}^{Z} \rightarrow AB^{H2\prime}$	20.3	26.9	8.6	7.6	29.7	1.5	2.9	18.6	2.3
$A_2{}^{Z} \rightarrow AB^{H2}$	22.4	12.6	4.1	9.4	15.7	3.3	3.5	10.5	2.9
$A_3{}^{Z} \rightarrow AB^{Ph1\prime}$	22.8	29.4	4.5	9.8	31.9	3.7	5.4	21.1	4.8
$A_2{}^{Z} \rightarrow AB^{Ph1}$	24.3	14.5	6.0	11.2	17.5	5.1	3.8	10.8	3.2
$A_1{}^{E} \rightarrow AB^{Ph2}$	24.5	11.1	6.2	11.1	14.5	5.0	5.8	8.5	5.2
$A_3{}^{Z} \rightarrow AB^{OH1}$	18.3	24.9	0.0	6.1	28.2	0.0	0.6	16.3	0.0
B^{H1}	17.2			4.0			−2.8		
B^{H2}	17.7			3.9			−3.1		
B^{Ph1}	19.0			5.8			−2.5		
B^{Ph2}	17.8			4.1			−2.6		
B^{OH1}	18.0			4.9			−3.2		
B^{OH2}	20.5			7.6			−1.3		
$B^{H1} \rightarrow BC^{H1}$	22.2	5.0		7.9	3.9		5.3	8.1	
$B^{H2} \rightarrow BC^{H2}$	22.2	4.5		12.2	8.3		7.9	11.0	
$B^{Ph1} \rightarrow BC^{Ph1}$	21.6	2.6		7.7	1.9		2.9	5.4	
$B^{Ph2} \rightarrow BC^{Ph2}$	20.2	2.4		6.3	2.2		2.8	5.4	
$B^{OH1} \rightarrow BC^{OH1}$	23.2	5.2		9.5	4.6		4.4	7.6	
$B^{OH2} \rightarrow BC^{OH2}$	28.1	7.6		14.6	7.0		8.9	10.2	
$A^{Z}{\cdot}BF_4{}^{-}{\cdot}MDA$	0.0[b]			0.0[b]			0.0[b]		
$A^{Z}{\cdot}BF_4{}^{-}{\cdot}MDA \rightarrow AB^{H}$	12.0	12.0		15.9	15.9		8.4	8.4	
B^{H}	11.9			15.1			5.8		
$B^{H} \rightarrow BC^{H}$	21.4	9.5		21.6	6.5		16.2	10.4	
$A^{Z}{\cdot}BF_4{}^{-}{\cdot}MDA$	0.0[b]			0.0[b]			0.0[b]		
$A^{Z}{\cdot}BF_4{}^{-}{\cdot}MDA \rightarrow AB^{Ph}$	17.5	17.5		21.5	21.5		11.8	11.8	
B^{Ph}	16.8			19.7			6.0		
$B^{Ph} \rightarrow BC^{Ph}$	24.3	7.5		27.1	7.4		16.1	10.1	

[a] Energy values are referred to $\mathbf{A^{Z}}$ + **MDA** (separated O-protonated benzaldehyde and methyldiazoacetate). [b] Energy values are referred to $\mathbf{A^{Z}{\cdot}BF_4{}^{-}{\cdot}MDA}$ (associated O-protonated benzaldehyde, methyldiazoacetate, and $BF_4{}^{-}$).

$\mathbf{AB^{H1}}$, the C–C bond distance is still rather long (2.24 Å), the C–N bond only slightly elongated in comparison with the free MDA. In $\mathbf{B^{Ph2}}$ the newly formed C–C bond is 1.59 Å and the C–N bond is 1.46 Å.

The migration of the phenyl group proceeds *via* transition state $\mathbf{BC^{Ph2}}$ to give the O-protonated ester aldehyde $\mathbf{C^{Ph}}$. This last step is also strongly exergonic by 40.5 kcal mol^{-1}. In $\mathbf{BC^{Ph2}}$ loss of one N_2 molecule is still proceeding (d_{C-N} = 1.76 Å), while

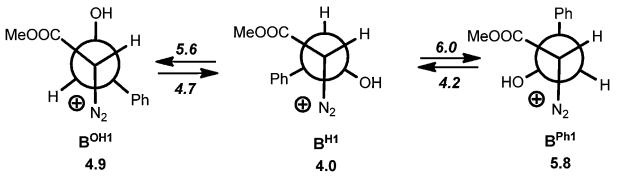

Scheme 6 Newman projections of all stable conformations with a 1*S*,2*S*-configuration after C–C bond formation between O-protonated benzaldehyde and MDA (free energies in kcal mol^{-1}, rotational barriers in italic).

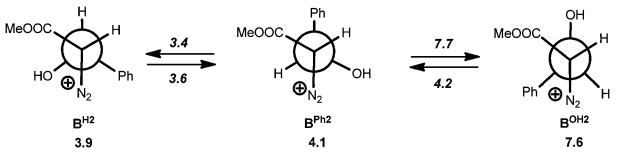

Scheme 7 Newman projections of all stable conformations with a 1*S*,2*R*-configuration after C–C bond formation between O-protonated benzaldehyde and MDA (free energies in kcal mol^{-1}, rotational barriers in italic).

at the same time the phenyl group starts to migrate between the two adjacent C-atoms ($d_{C–C(Ph)}$ = 1.53 and 2.35 Å). The free energy of activation associated with this path is merely 2.2 kcal mol^{-1} and, thus, slightly lower than the one obtained for the formation of the protonated β-ketoester $\mathbf{C^H}$ (3.9 kcal mol^{-1}). After deprotonation of the ester aldehyde $\mathbf{C^{Ph}}$ that molecule rapidly tautomerizes to yield the thermodynamically more stable respective 3-hydroxyacrylate **II**.

Besides rotamers $\mathbf{B^{H1}}$ and $\mathbf{B^{Ph2}}$, obtained from $\mathbf{A_1}$, in principle four other rotamers could be formed either directly from $\mathbf{A_2}$ and $\mathbf{A_3}$ or *via* rotation about the newly formed C–C bonds of $\mathbf{B^{H1}}$ and $\mathbf{B^{Ph2}}$, respectively. Newman projections of all stable conformations are depicted in Schemes 6 and 7 including the free energy barriers of their interconversions (numbers in italic).

DFT calculations reveal that the formation of all rotamers with OH and COOMe substituents in a synclinal orientation originates from the associated species $\mathbf{A_2}$ and $\mathbf{A_3}$. Free energy profiles for the coupling of associated O-protonated benzaldehyde and MDA to afford the rotamers $\mathbf{B^{H2}}$, $\mathbf{B^{Ph1}}$, and $\mathbf{B^{OH1}}$ are shown in Schemes 8–10. Intermediate $\mathbf{B^{OH2}}$, which is the least stable intermediate, is apparently not formed directly, since we were unable to locate a transition state $\mathbf{TS_{AB}^{OH2}}$. The kinetic barrier for the formation of these intermediates, when starting from $\mathbf{A_3}^{Z}$ is 29.7, 31.9, and 28.2 kcal mol^{-1}, respectively. On the other hand, in the case of $\mathbf{A_2}^{Z}$ the free energies of activation are considerably lower being 15.7 and 17.5 kcal mol^{-1}, respectively.

Alternatively, rotamers $\mathbf{B^{Ph1}}$, $\mathbf{B^{OH1}}$, $\mathbf{B^{H2}}$ and $\mathbf{B^{OH2}}$ are readily accessible from $\mathbf{B^{H1}}$ and $\mathbf{B^{Ph2}}$, respectively, *via* rotation of the internal C–C bond by 120° (Schemes 6 and 7) since the rotational barriers are small being in the range of 3.4 to 7.7 kcal mol^{-1}. Once formed, intermediates $\mathbf{B^{Ph1}}$ and $\mathbf{B^{H2}}$ are able to undergo phenyl and hydride migration, respectively, leading eventually to the formation of 3-hydoxyacrylate **II** and β-ketoester **I** (Schemes 8 and 9). The free energy of activation for these processes is 1.9 and 8.3 kcal mol^{-1} and phenyl migration is thus strongly favored over hydride migration. On the other hand, intermediate $\mathbf{B^{OH1}}$ (and $\mathbf{B^{OH2}}$), with the OH and N_2 substituents in an antiperiplanar position, undergoes a facile 1,2-OH-migration with a free energy barrier of 4.6 kcal mol^{-1} (7.0 kcal mol^{-1} in the case of $\mathbf{B^{OH2}}$) leading to the stable carbenium ion $\mathbf{C^{OH}}$ (Scheme 11). Under these reaction conditions (10 mol% HBF_4, CH_2Cl_2 as the solvent) the formation of epoxide **III** was not

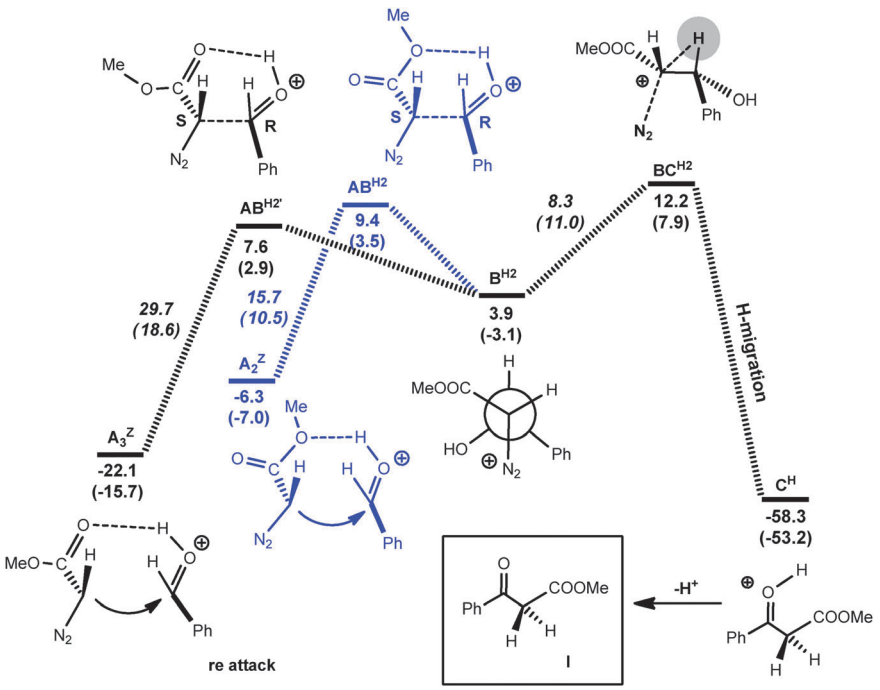

Scheme 8 Proton catalyzed coupling of O-protonated benzaldehyde and MDA originating from the associated species $\mathbf{A_2}^{Z}$ and $\mathbf{A_3}^{Z}$ forming rotamer $\mathbf{B^{H2}}$ *via re* face attack and subsequent H-migration to give β-ketoester **I**. The free energy values (kcal mol^{-1}) are referred to $\mathbf{A}^{Z}$ + **MDA**, numbers in parentheses refer to solvent-corrected free energies, solvent = CH_2Cl_2.

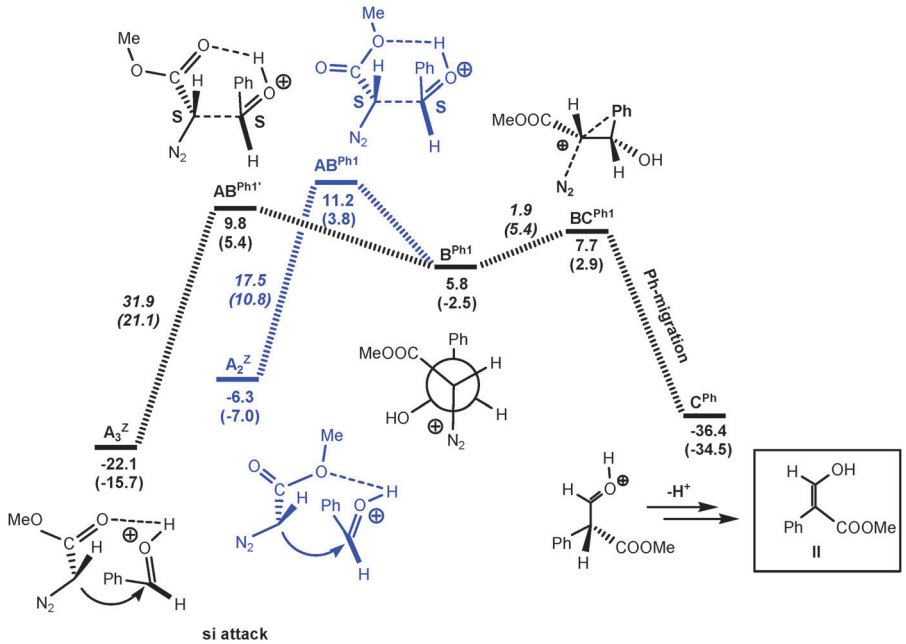

Scheme 9 Proton catalyzed coupling of O-protonated benzaldehyde and MDA originating from the associated species $\mathbf{A_2}^{Z}$ and $\mathbf{A_3}^{Z}$ forming rotamer $\mathbf{B}^{Ph1}$ *via si* face attack and subsequent Ph-migration to give hydroxyacrylate **II**. The free energy values (kcal mol^{-1}) are referred to $\mathbf{A}^{Z}$ + **MDA**, numbers in parentheses refer to solvent-corrected free energies, solvent = CH_2Cl_2.

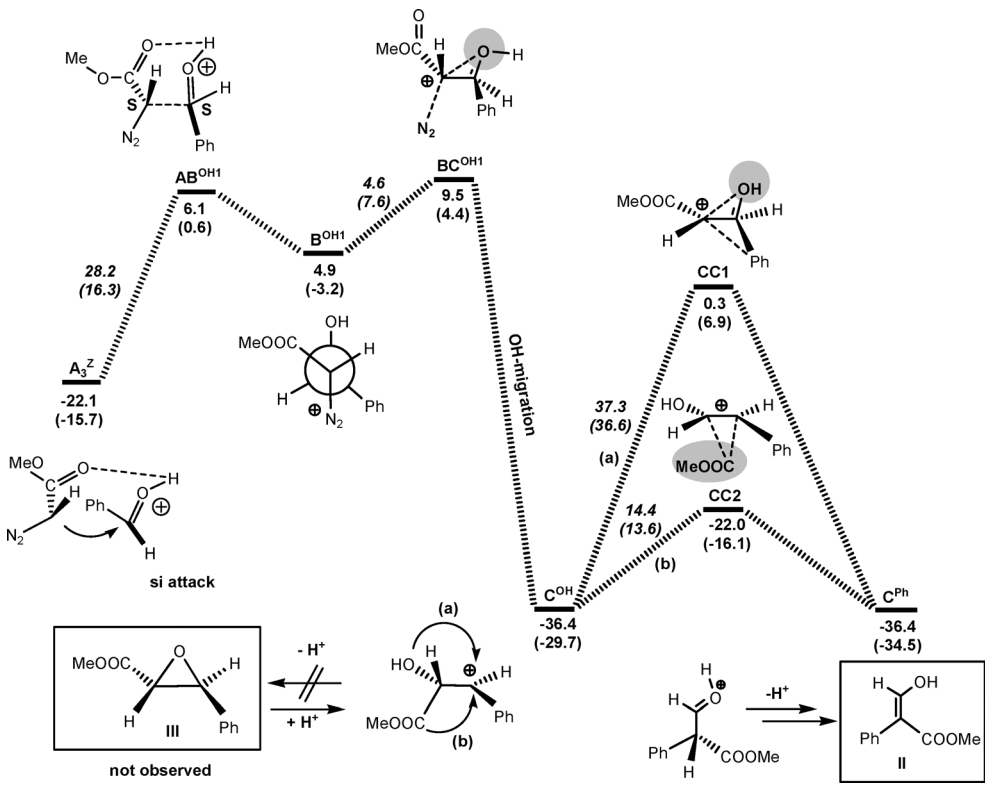

Scheme 10 Proton catalyzed coupling of O-protonated benzaldehyde and MDA *via si* face attack followed by O-migration giving hydroxacrylate **II**. The free energy values (kcal mol^{-1}) are referred to $\mathbf{A}^{Z}$ + **MDA**, numbers in parentheses refer to solvent-corrected free energies, solvent = CH_2Cl_2.

observed. In fact, in the presence of strong acids the opposite reaction, *viz*. epoxide ring opening, is easily achieved yielding 1,2-difunctional systems.[17] However, in the absence of potential nucleophiles, *e.g*., a coordinating counterion or a coordinating solvent as in the present case, it is well known that rearrangement reactions may take place to give aldehydes, ketones, or alkenes.[18] DFT calculations reveal that protonated epoxide **III** is unstable spontaneously undergoing ring opening to give $\mathbf{C}^{OH}$.

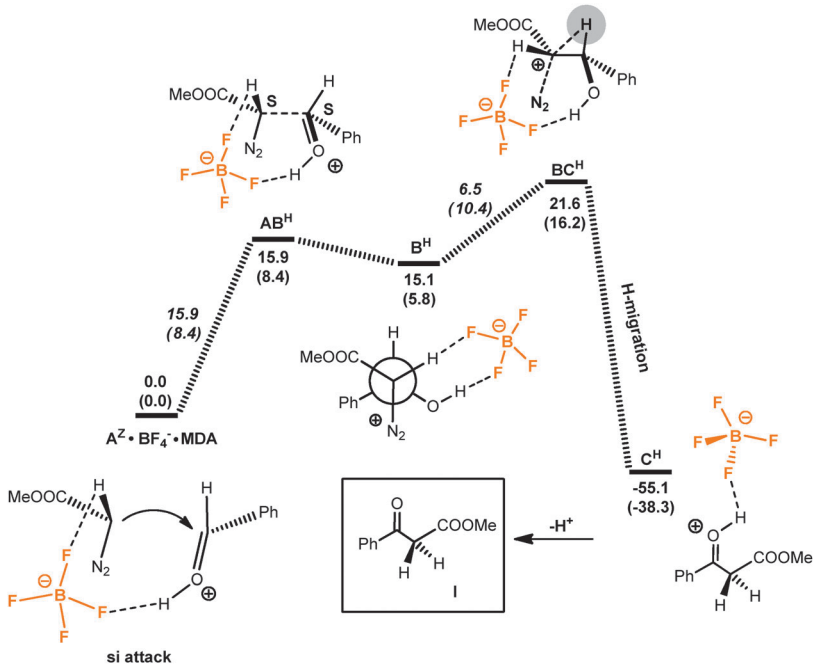

Scheme 11 Proton catalyzed and BF_4^- assisted coupling of O-protonated benzaldehyde and MDA originating from the associated species $\mathbf{A^Z \cdot BF_4^- \cdot MDA}$. The free energy values (kcal mol^{-1}) are referred to $\mathbf{A^Z \cdot BF_4^- \cdot MDA}$, numbers in parentheses refer to solvent-corrected free energies, solvent = CH_2Cl_2.

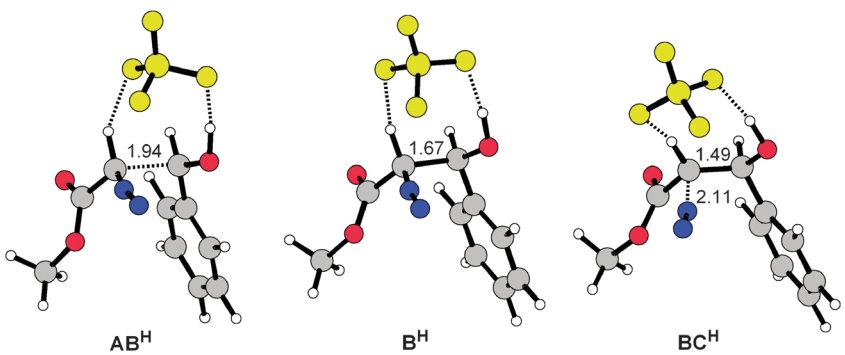

Fig. 2 Optimized B3LYP geometries of the equilibrium structures and transition states for the anion-assisted pathway (distances in Å).

Therefore, $\mathbf{C^{Ph}}$ could be also formed *via* concerted OH- and phenyl-migration (path a) or *via* a 1,2-shift of the COOMe substituent (path b). However, the free energy of activation for the first is prohibitively high being 37.3 kcal mol^{-1}, whereas the energy barrier for the latter is merely 14.4 kcal mol^{-1} and could be an alternative facile mechanism for the formation of $\mathbf{C^{Ph}}$ and subsequently 3-hydoxyacrylate **II**. For comparison, the barriers for H-, Ph-, and OH-migration are in the range of 1.9 to 8.3 kcal mol^{-1}.

If we assume that the associated species $\mathbf{A_1}$, $\mathbf{A_2}$, and $\mathbf{A_3}$ can interconvert rapidly (fast pre-equilibria) with respect to the subsequent C–C bond forming reactions, Curtin–Hammett conditions will apply.[19] Accordingly, the competition between mechanisms will be controlled by the free energy difference ($\Delta\Delta G^{\ddagger}$) between the highest barriers in the first intermediate-forming reactions rather than the barriers ($\Delta G^{\ddagger}$) themselves. In this respect, C–C bond formation originating from $\mathbf{A_3^Z}$ to afford $\mathbf{B^{OH1}}$ *via* transition state $\mathbf{AB^{OH1}}$ is slightly more favorable than the respective C–C coupling reactions starting from associates $\mathbf{A_1}$ and $\mathbf{A_2}$, respectively, *i.e.*, this reaction takes place at a faster rate (however, $\Delta\Delta G^{\ddagger}$ ranges merely from 1.5–5.1 kcal mol^{-1}, see Table 1).

The selectivity determining step is the migration of the H-, Ph-, and OH-substituents in intermediates **B**. In agreement with experimental data, Ph-migration is slightly favored over H- and OH-migration and thus the formation of 3-hydroxy-acrylates (**II**) over β-ketoesters (**I**).

Finally, we also considered the involvement of the counterion BF_4^-. A free energy profile for the counterion assisted the coupling of O-protonated benzaldehyde and MDA *via si*-face attack giving rotamer $\mathbf{B^H}$ and subsequent H-migration is presented in Scheme 11 (a similar profile is found for the BF_4^- assisted formation of rotamer $\mathbf{B^{Ph}}$ and subsequent Ph-migration, see Table 1). Optimized structures of intermediates and transition states are depicted in Fig. 2. The overall reaction is similar to the "BF_4^--free" pathway (Scheme 4) but the presence of the BF_4^- anion seems to raise all energy barriers even if the solvent is included in the calculations. The barrier of the C–C bond forming step to yield $\mathbf{B^H}$ is

15.9 kcal mol^{-1} (*cf.* 13.5–15.7 kcal mol^{-1} for the "BF_4^--free" pathway, 21.5 kcal mol^{-1} for the formation of $\mathbf{B^{Ph}}$). Hydride migration is not affected by the presence of the counterion and proceeds readily *via* $\mathbf{BC^H}$ to give $\mathbf{C^H}$. The free energy of activation is 6.5 kcal mol^{-1} (3.8–8.3 kcal mol^{-1} for the "BF_4^--free" pathway, 7.4 kcal mol^{-1} for the formation of $\mathbf{C^{Ph}}$ *via* Ph migration).

The above results suggest that Brønsted acids with non-nucleophilic counter anions such as $BAr'_4{}^-$ (Ar′ = 3,5-$C_6H_3(CF_3)_2$)—although experimentally not tested—or poorly coordinating anions such as BF_4^- should give the best results. This is in agreement with experimental data revealing that with HBF_4 (in the form of $HBF_4{\cdot}Et_2O$) the best results could be achieved, while with H_2SO_4, HCl, or CH_3COOH only small or trace amounts of products were obtained.[8] In fact, the use of more conventional Brønsted acids with nucleophilic anions such as HSO_4^-, Cl^- or CH_3COO^- as well as coordinating (nucleophilic) solvents may lead to side reactions and thus to poor or no yields of **I** and **II**, respectively. For instance, the carbenium intermediate $\mathbf{C^{OH}}$ would readily form the respective 1,2-difunctional products.

Conclusions

Protons, in the form of the Brønsted acid $HBF_4{\cdot}Et_2O$ in CH_2Cl_2 as the solvent, catalyze the reaction between aromatic aldehydes and ethyldiazoacetate to provide β-keto esters (**I**) and 3-hydroxyacrylates (**II**). A conceivable mechanism for the proton catalyzed coupling of benzaldehyde and methyldiazoacetate (MDA) as model substrates was established by means of DFT/B3LYP calculations where the chemoselectivity is rationalized. In CH_2Cl_2 solution, MDA and O-protonated benzaldehyde form hydrogen bonded associates. Pathways with the lowest energy barriers originate from such adducts yielding upon nucleophilic attack of MDA at the *si*- or *re*-face of the O-protonated aldehyde various rotamers—diastereomers with 1*S*,2*S*- and 1*S*,2*R*-configurations, respectively. The C–C bond formation is the rate determining step. In all stable rotamers, the H, Ph, and OH substituents are in an antiperiplanar orientation with respect to the N_2-substituent. This arrangement is a prerequisite for the subsequent 1,2-migration of H-, Ph-, and OH-substituents, the key step as chemoselectivity is concerned, to give **I** and **II**, respectively. Calculations indicate that the formation of **II** is slightly favored over the formation of **I** (*ca.* 2 : 1 ratio). For comparison, in iron catalyzed versions of this process utilizing complexes $[FeCp(CO)_2(THF)]BF_4$, $[Fe(PNP)(CO)(CH_3CN)_2](BF_4)_2$, and $[Fe(PNP)(CO)_2(Cl)]BF_4$ as pre-catalysts the formation of **II** is strongly favored over the formation of **I**.[5–7] Epoxide formation is not feasible in the presence of an acid with a non-nucleophilic counterion since spontaneous ring opening takes place. Moreover, a BF_4^--assisted pathway has been also taken into account. Interestingly, both the C–C bond forming step and the hydride migration were found to be in the same order of magnitude than for the analogous "BF_4^--free" reactions. Accordingly, Brønsted acids with non-nucleophilic counterions, *e.g.*, $BAr'_4{}^-$ (Ar′ = 3,5-$C_6H_3(CF_3)_2$)—although experimentally not tested—or the poorly coordinating anion BF_4^- (experimentally used) should indeed give the best results, while more conventional Brønsted acids with nucleophilic anions such as Cl^- or CH_3COO^- should result in poor or no conversions due to the diminished electrophilicity of the H^+ cation and/or side reactions with reactive carbenium intermediates.

References

1 (*a*) C. R. Holmquist and E. J. Roskamp, *J. Org. Chem.*, 1989, **54**, 3258; (*b*) C. R. Holmquist and E. J. Roskamp, *Tetrahedron Lett.*, 1992, **33**, 1131.
2 (*a*) A. Padwa, S. F. Hornbuckle, Z. Zhang and L. Zhi, *J. Org. Chem.*, 1990, **55**, 5297; (*b*) S. G. Sudrik, B. S. Balaji, A. P. Singh, R. B. Mitra and H. R. Sonawane, *Synlett*, 1996, 369.
3 K. Nomura, T. Iida, K. Hori and E. Yoshii, *J. Org. Chem.*, 1994, **59**, 488.
4 S. Kanemasa, T. Kanai, T. Araki and E. Wada, *Tetrahedron Lett.*, 1999, **40**, 5055.
5 (*a*) S. J. Mahmood and M. M. Hossain, *J. Org. Chem.*, 1998, **63**, 3333; (*b*) S. J. Mahmood, C. Brennan and M. M. Hossain, *Synthesis*, 2002, 1807.
6 D. Benito-Garagorri, J. Wiedermann, M. Pollak, K. Mereiter and K. Kirchner, *Organometallics*, 2007, **26**, 217.
7 L. G. Alves, G. Dazinger, L. F. Veiros and K. Kirchner, *Eur. J. Inorg. Chem.*, 2010, 3160.
8 M. E. Dudley, Md. M. Morshed, C. L. Brennan, M. S. Islam, M. S. Ahmad, M.-R. Atuu, B. Branstetter and M. M. Hossain, *J. Org. Chem.*, 2004, **69**, 7599.
9 T. Ye and M. A. McKervey, *Chem. Rev.*, 1994, **94**, 1091.
10 M. J. Frisch, *et al.*, *Gaussian 09, Revision A.02*, Gaussian, Inc., Wallingford, CT, 2009.
11 (*a*) A. D. Becke, *J. Chem. Phys.*, 1993, **98**, 5648; (*b*) B. Miehlich, A. Savin, H. Stoll and H. Preuss, *Chem. Phys. Lett.*, 1989, **157**, 200; (*c*) C. Lee, W. Yang and G. Parr, *Phys. Rev. B*, 1988, **37**, 785.
12 (*a*) A. D. McLean and G. S. Chandler, *J. Chem. Phys.*, 1980, **72**, 5639; (*b*) R. Krishnan, J. S. Binkley, R. Seeger and J. A. Pople, *J. Chem. Phys.*, 1980, **72**, 650; (*c*) A. J. H. Wachters, *Chem. Phys.*, 1970, **52**, 1033; (*d*) P. J. Hay, *J. Chem. Phys.*, 1977, **66**, 4377; (*e*) K. Raghavachari and G. W. Trucks, *J. Chem. Phys.*, 1989, **91**, 1062; (*f*) R. C. Binning and L. A. Curtiss, *J. Comput. Chem.*, 1995, **103**, 6104; (*g*) M. P. McGrath and L. Radom, *J. Chem. Phys.*, 1991, **94**, 511.
13 (*a*) V. Barone and M. Cossi, *J. Phys. Chem. A*, 1998, **102**, 1995; (*b*) J. Tomasi and M. Persico, *Chem. Rev.*, 1994, **94**, 2027.
14 A. V. Marenich, C. J. Cramer and D. G. Truhlar, *J. Phys. Chem. B*, 2009, **113**, 6378.
15 (*a*) M. Brookhart, G. C. Levy and S. Winstein, *J. Am. Chem. Soc.*, 1967, **89**, 1735; (*b*) G. A. Olah, D. H. O'Brien and M. Calin, *J. Am. Chem. Soc.*, 1967, **89**, 3582.
16 G. A. Olah, G. Rasul, C. York and G. K. S. Prakash, *J. Am. Chem. Soc.*, 1995, **117**, 11211.
17 (*a*) O. Mitsunobu, in *Comprehensive Organic Synthesis*, ed. B. M. Trost, L. Fleming and G. Pattenden, Pergamon Press, Oxford, 1990, vol. 6, pp. 88–93; (*b*) T. N. Birkinshaw, in *Comprehensive Organic Functional Group Transformations*, ed. A. R. Katrisky, O. Meth-Cohn, C. W. Rees and S. M. Roberts, Pergamon Press, Oxford, 1990, vol. 1, pp. 204–220.
18 (*a*) J. Picione, S. J. Mahmood, A. Gill, M. Hilliard and M. H. Hossain, *Tetrahedron Lett.*, 1998, **39**, 2681; (*b*) R. D. Bach and J. M. Domagala, *J. Org. Chem.*, 1984, **49**, 4181.
19 For a general treatment of the Curtin–Hammett principle, see: J. I. Seeman, *Chem. Rev.*, 1983, **83**, 83.

